

Solute migration and microstructure evolution of the hypereutectic Cu-73.4 wt.% Ag alloy during directional solidification under high-gradient magnetic fields

Jinmei Sun^{1,2}, Baoze Zhang^{1,3}, Tie Liu^{1,*}, Tianru Zhou^{1,3}, Noriyuki Hirota⁴, Qiang Wang¹

1. Key Laboratory of Electromagnetic Processing of Materials (Ministry of Education),

Northeastern University, Shenyang 110819, China

2. School of Materials Science and Engineering, Northeastern University, Shenyang 110819, China

3. School of Metallurgy, Northeastern University, Shenyang 110819, China

4. Research Center for Fundamental Materials, National Institute for Materials Science, Tsukuba

305-0003, Japan

Address correspondence to E-mail: liutie@epm.neu.edu.cn

Abstract:

During preparation of metallic material, solute migration has a significant effect on the microstructure. High magnetic field has an enormous potential on controlling alloy solidification on the basis of Lorentz force, magnetic force, etc. In this work, directional solidification experiments of a Cu-73.4 wt.% Ag alloy have been conducted under different gradient magnetic fields. The effects of gradient magnetic fields on the solute migration and microstructure evolution of the alloys during the directional solidification process have been investigated. Without magnetic field, the alloy showed an aligned dendritic microstructure. Under a uniform magnetic field, the dendritic microstructure transformed to a eutectic morphology. Under a gradient magnetic field, the alloy exhibited again the dendritic microstructure, but with poor alignment. The transformation of the microstructure from aligned dendritic to eutectic to poor aligned dendritic morphology can be attributed to the combining effects of the Lorentz force and magnetic force on the migration of Cu solute at the solid/liquid interface. The

1 results of this work provide a new insight to regulating the microstructure of alloys
2 using high gradient magnetic fields.
3
4
5

6 **1. Introduction**

8 During the solidification process of alloys, the solute migration and distribution
9 behavior at the solid/liquid interface and in the mushy zone determine the crystal
10 growth and microstructure evolution [1]. For example, Zhang et al. [2] simulated the
11 eutectic growth and found that the interlamellar spacing was increased by the
12 convection, which promoted solute migration. Yan et al. [3] evidenced that the solute
13 enrichment at the solid/liquid interface during the solidification of an Al-Fe alloy
14 caused a constitutional undercooling and induced the planar-cellular-dendritic crystal
15 growth pattern transition. According to the solidification of a dilute binary alloy,
16 Mullins et al. [4] proposed the theory of interface stability, which stated that the
17 diffusion of solutes affected the stability of the planar interface. Ma et al. [5] simulated
18 the solidification of binary alloys and suggested that the shrinking flow in the mushy
19 zone resulted in a solute enrichment and caused serious local segregation and
20 solidification cracks. Therefore, it is of great importance to control the solute migration
21 behavior at the solid/liquid interface and in the mushy zone during the solidification
22 process of alloys.
23
24
25
26
27
28
29
30
31
32
33
34
35
36
37
38
39
40

41 Various solidification technologies have been developed to modify the solute migration
42 behavior and thus regulate the microstructure and properties of materials, such as
43 directional solidification technology [6], deep undercooling technology [7], rapid
44 solidification technology [8], and external field-assisted solidification technology [9].
45 Among them, high magnetic field has attracted much attention due to its potential on
46 controlling alloy solidification on the basis of Lorentz force, thermoelectric magnetic
47 force (a special kind of the Lorentz force), magnetization force, etc. [10-13]. In a
48 uniform magnetic field, the movement of an electrically conducting fluid will cause an
49 electric current, the Lorentz force will be produced by the interaction of the current and
50
51
52
53
54
55
56
57
58
59
60

the applied magnetic field. Keigo [14] applied a uniform magnetic field upon the growth of single-crystal silicon semiconductor, the impurities were effectively eliminated by the Lorentz force, which suppressed the convection and stabilized the solid-liquid interface. In addition, if the thermoelectric current is induced by the difference of Seebeck coefficient between the liquid and solid at a liquid/solid interface, the thermoelectric magnetic force will be produced by the interaction of the current and the applied uniform magnetic field. In contrast to the Lorentz force, researchers have evidenced that the thermoelectric magnetic force could promote the convection in the mushy zone and result in dendrite fragmentation [15, 16]. They further evidenced that such dendrite fragmentation could promote the columnar-to-equiaxed transition and thus refine the microstructure [15]. Furthermore, in a gradient magnetic field, the magnetization force will be induced by the interaction of the magnetization of materials and the imposed magnetic field gradient [17]. The authors have confirmed that the magnetization force has a significant ability to control solute migration and produced Mn-Sb [18] and Tb-Dy-Fe [19] composites with compositional gradients throughout the composites based on such controlling.

Above studies have showed that the Lorentz force or thermoelectric magnetic force or magnetization force alone can significantly affect the solute migration and microstructure of the alloys. However, depending on the conditions of the magnetic field gradient and solidification, these forces may perform combined action upon the solidification process [20-22]. Thus, the effects of the corporate action of these forces on the solute migration and microstructure need to be clarified.

In this work, the hypereutectic Cu-73.4 wt.% Ag alloy was selected as a model alloy to investigate the effect of gradient magnetic fields on the solute migration and microstructure evolution during the directional solidification of the alloy. As an alloy with high conductivity and strength, the Cu-Ag alloy is widely used in various fields, such as electronics, transportation, and machinery manufacturing. Cu and Ag are both

antimagnetic [23, 24]. Ag has a higher magnetic susceptibility than that of Cu. According to the Ag-Cu phase diagram (Fig. 2(a)), the equilibrium microstructure of the Cu-73.4 wt.% Ag alloy consists of primary Ag phase and eutectic Cu and Ag phases. Directional solidification experiments of the alloy under different gradient magnetic fields were conducted. The microstructure, solid/liquid interface morphology, solute distribution, and phase content of the alloy were investigated, and the mechanism of the effect of high gradient magnetic fields on solidification was analyzed.

2. Experimental

Cu and Ag particles with a purity of 99.99% were selected to prepare a Cu-73.4 wt.% Ag master alloy using a vacuum induction melting furnace. The uniformity of the alloy composition and microstructure was confirmed by chemical analysis and microstructure observation. The master alloy was cut into $\Phi 6 \text{ mm} \times 100 \text{ mm}$ cylindrical rods. The rods were then placed in a graphite crucible (inner diameter 6.5 mm; outer diameter 8 mm) for directional solidification experiments. An equipment under a high magnetic field was used for the directional solidification and quenching experiments. The equipment consisted of a superconducting magnet and a Bridgman directional solidification furnace [25]. The schematic diagram of the equipment is shown in Fig. 1(a). The furnace was evacuated to $2 \times 10^{-3} \text{ Pa}$, and then 350 Pa of argon gas was introduced as a protective gas. According to the phase diagram of the Cu-Ag system, its eutectic temperature is 779°C. To ensure superheating during solidification, the temperature was increased to 1100°C at a rate of 10 °C/min and held at this temperature for 30 min to achieve a steady temperature inside the alloy. Then, the samples were pulled down 20 mm to the liquid Ga-In-Sn at pulling velocities of 100 $\mu\text{m/s}$ for directional solidification, followed by quenching to preserve the solid-liquid interface. The solidification direction (v) was upward and parallel the long axis of the samples (z). The temperature and atmosphere remained unchanged during directional solidification and quenching experiments. The product of the magnetic flux density (B) and its gradient (dB/dz), BdB/dz , was used to characterize the magnetic field gradient effects.

4 magnetic field gradients, i.e., 0 T and 0 T²/m, 5.31 T and 0 T²/m, 5.31 T and -30 T²/m, and 5.31 T and -70 T²/m were chosen by fixing the samples at different positions in the bore of the superconducting magnet (Figs. 1(b) and (c)).

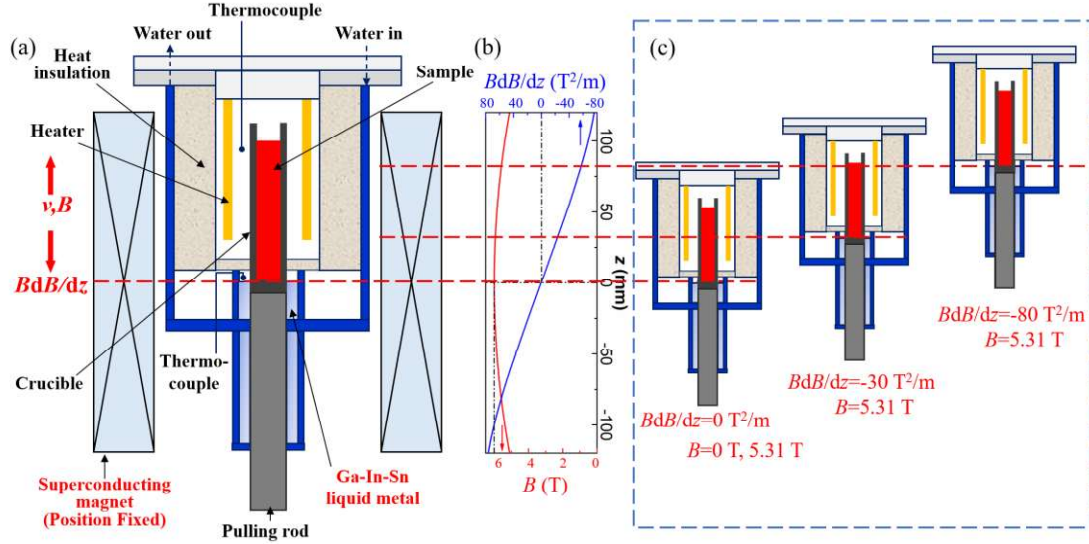


Fig. 1 Schematic of the experimental apparatus and the magnetic flux density distribution curve. (a) schematic of experimental apparatus, (b) distribution curves of B and BdB/dz , (c) showing the positions where the samples were placed in the magnet. The direction of z -axis in (b) corresponds to the vertical upward direction in (a).

After the experiments, the samples with an effective length about 95 mm were cut horizontally and vertically along the solidification direction (high magnetic field direction). Both surfaces of the cut samples were polished mechanically by 80# ~ 5000# sandpapers and Colloidal Silica Slurry, and then etched for metallographic analysis. The etching solution comprised of 2 g FeCl₃, 5 ml HCl, and 100 ml C₂H₅OH. The microstructure morphology was observed by optical microscopy (OM, DSX500, Olympus) and scanning electron microscopy (SEM, Sigma 300, Zeiss). The various phase components were identified by energy dispersive spectroscopy (EDS, Ultim Max, Oxford Instruments). Point scanning, line scanning, and mapping were performed by electron probe micro-analysis (EPMA, JAX-8530F, JEOL). Line scanning of Cu was performed to determine the solute distribution at the solid/liquid interface. Point scanning of the dendritic tips at the solid/liquid interface was performed to calculate the solute distribution coefficient. The point measurements were performed from the

solid phase to the liquid phase zones, with a total of 15 points and a step size of 1 μm . Mapping of the dendritic tip position at the solid/liquid interface was performed to determine the solute distribution in the solute diffusion layer. Quantitative analysis of the content of the Ag phase in the directional solidification zone was performed with Image Pro Plus software. The area fraction of the Ag phase was measured from the solidification starting surface to the solid/liquid interface. Each value was measured five times, and the average value was calculated. The area fraction was used to estimate the volume fraction.

3. Results and Discussion

The microstructure of the Cu-73.4 wt.% Ag master alloy is shown in Figs. 2(b) and (c). It is composed of a dark gray matrix and a white dendritic structure. An enlargement of the dark gray matrix enclosed by the red square in Fig. 1(b), which is a layered eutectic structure, is shown in Fig. 1(c). The EDS results about the dendritic phase and matrix are shown in Figs. 2(d) and (e). Combining the Ag-Cu diagram (Fig. 1(a)) and EDS patterns (Fig. 1(d) and (e)), it can be concluded that the white dendrites are the primary Ag phase and the dark gray matrix is the Cu-Ag eutectic.

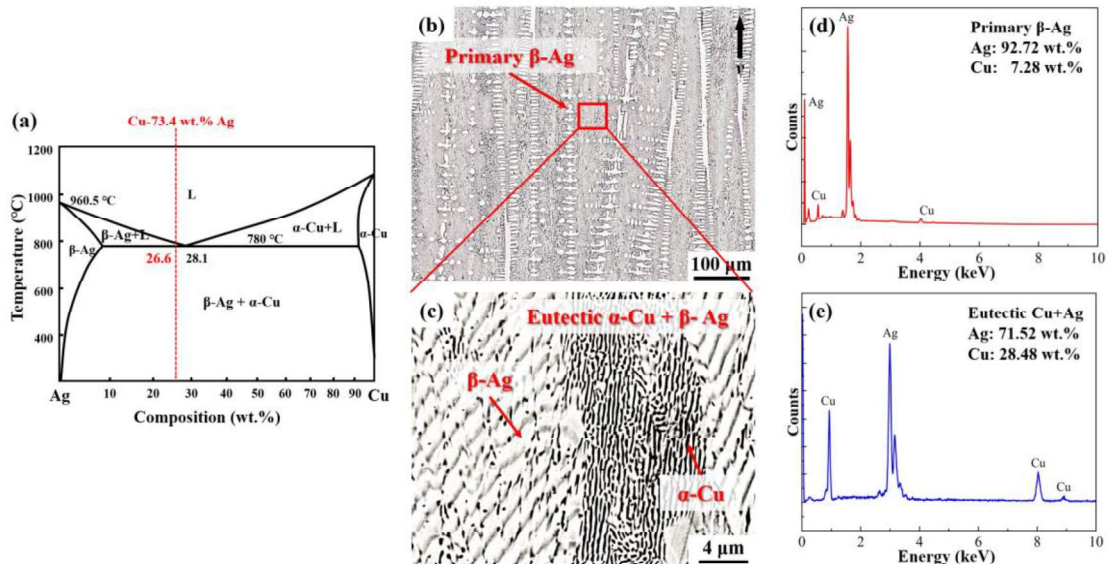


Fig. 2 Microstructure of the Cu-73.4 wt.% Ag alloy and the corresponding phase-composition patterns: (a) phase diagram, (b) primary phase structure (250x), (c) eutectic phase structure (3500x), (d) EDS pattern of the primary Ag phase, and (e) EDS pattern of the Cu-Ag eutectic.

The OM images of panoramic and local magnified microstructures of horizontal sections of the alloys are shown in Fig. 3. Without magnetic field, the directional solidification zone was uniformly distributed with primary Ag dendrites along the solidification direction and fine Cu-Ag eutectic, i.e., a hypereutectic microstructure (Fig. 3(a)). With a uniform magnetic field (5.31 T, 0 T²/m), the primary Ag dendrites transformed into Cu-Ag eutectic structures (Figs. 3(b-b2)). While with a low gradient magnetic field (5.31 T, -30 T²/m), the Cu-Ag eutectic structure transformed back to the hypereutectic microstructure, i.e., a mixture of primary Ag dendrite and Cu-Ag eutectic, although the direction of long axis of dendrites was relative random (Fig, 3(c)). With the increase of the field gradient from -30 T²/m to -70 T²/m, the content and directional growth degree of the primary Ag dendrites increased (Figs. 3(c) and (d)). The above observations indicate that as the uniform magnetic field and gradient magnetic field were applied, the microstructure of the Cu-73.4 wt.% Ag alloy underwent a transition from a hypereutectic to a eutectic to a hypereutectic. The microstructures of vertical sections of the alloys have confirmed such transition (Fig. 4).

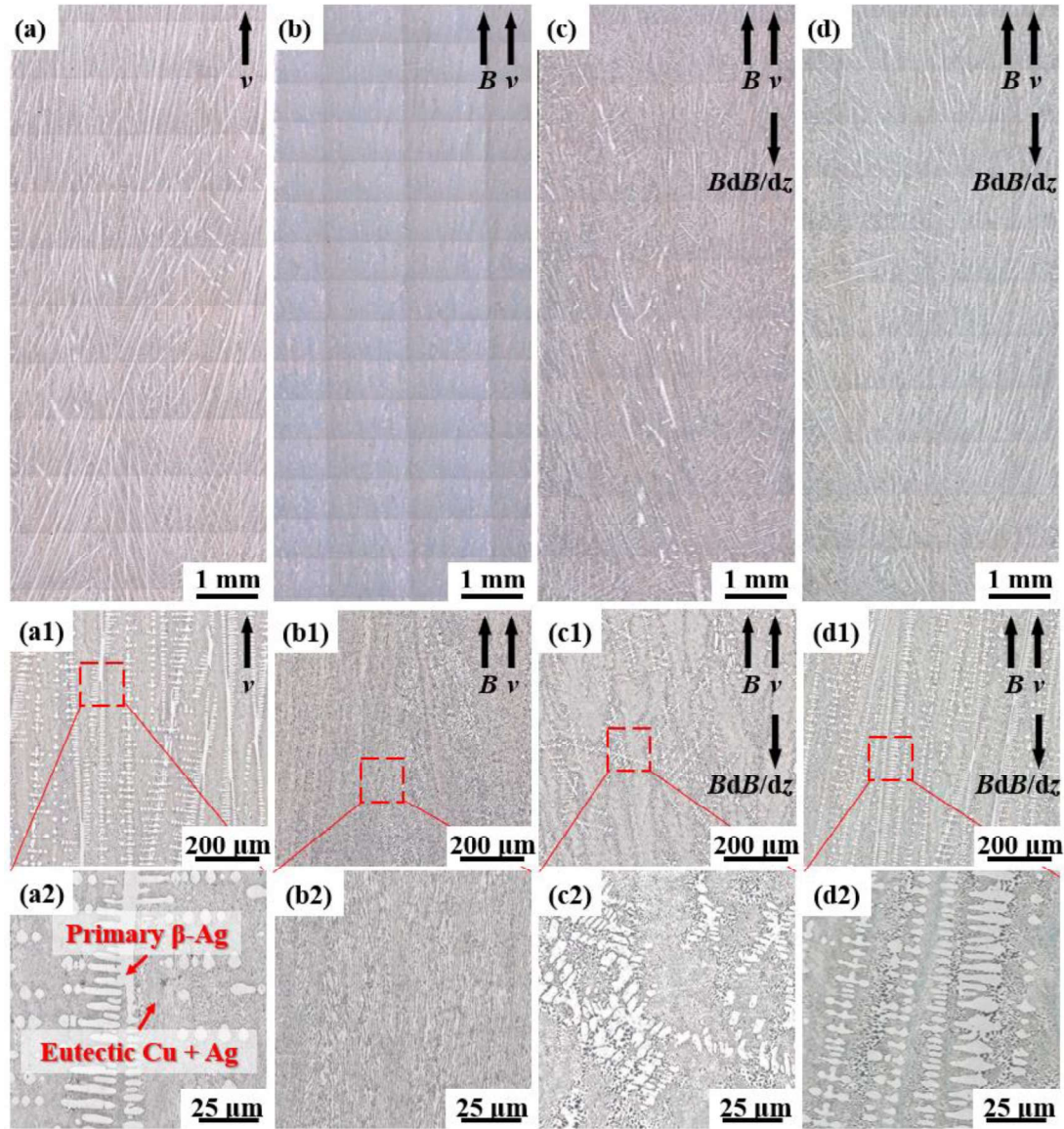


Fig. 3 Panoramic microstructure (30x) and local magnified microstructure (130x and 500x) of the horizontal section of the Cu-73.4 wt.% Ag alloy directionally solidified under different magnetic fields: (a-a2) (0 T, 0 T²/m), (b-b2) (5.31 T, 0 T²/m), (c-c2) (5.31 T, -30 T²/m), and (d-d2) (5.31 T, -70 T²/m).

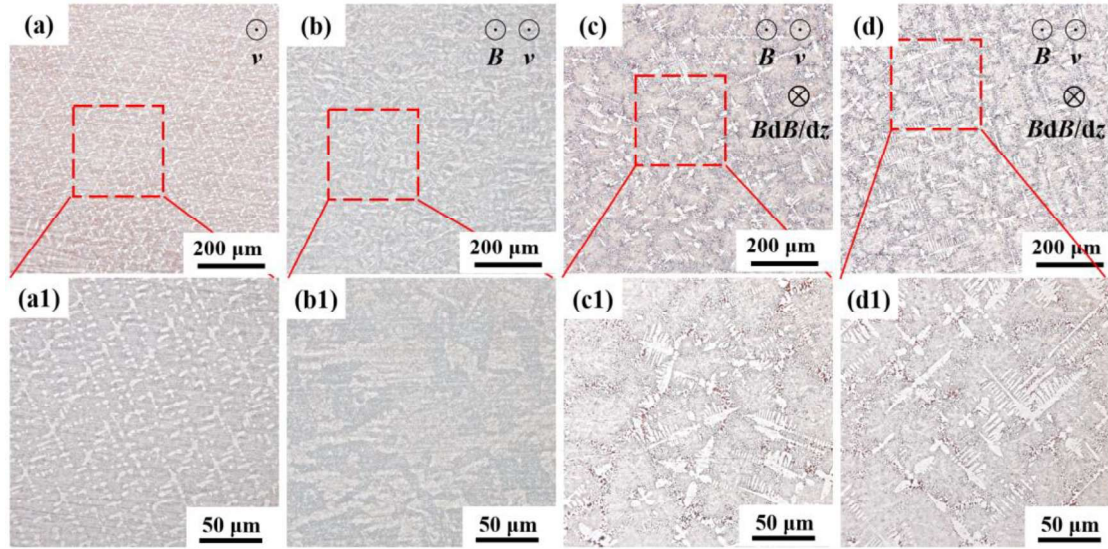


Fig. 4 Microstructure (130x) and local magnified microstructure (250x) of the vertical section of the Cu-73.4 wt.% Ag alloy directionally solidified under different magnetic fields: (a) and (a1) (0 T, 0 T²/m), (b) and (b1) (5.31 T, 0 T²/m), (c) and (c1) (5.31 T, -30 T²/m), and (d) and (d1) (5.31 T, -70 T²/m).

The distributions of the primary Ag phase in the directional solidification zones of the samples are shown in Fig. 5. Without magnetic field, the distribution of the primary phase was relatively uniform. With the uniform magnetic field (5.31 T, 0 T²/m), a line with a value of 0 indicated that no primary Ag phase was observed throughout the sample. While with a low gradient magnetic field (5.31 T, -30 T²/m), the amount of the primary Ag phase was lower than that of the without magnetic field case. In addition, its content fluctuated along the axial direction. When the magnetic field gradient increased to -70 T²/m, the content of the primary Ag phase was similar to that without magnetic field case, although it still showed relatively slight fluctuations along the axial direction. The volume fraction distributions of the primary Ag phase further confirmed the results of the microstructure observation.

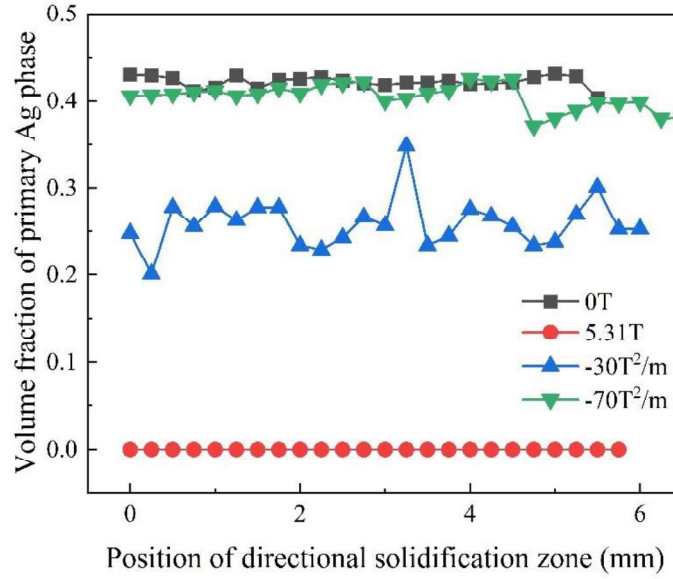


Fig. 5 Volume fractions of the primary Ag phase in the directional solidification zone of the Cu-73.4 wt.% Ag alloy directionally solidified under different magnetic fields.

To investigate the solute migration mechanism, quenching experiments were conducted during the directional solidification process, and the morphology of the solid/liquid interface was fixed. The microstructures of the solid/liquid interface of the quenched alloys are shown in Fig. 6. To characterize the degree of the directional growth of the primary Ag dendrites, the angle (i.e. θ) between the growth direction of the long axis of the dendrites and the direction of the directional solidification or high magnetic field was measured. For directional solidification at (0 T, 0 T²/m), the solid/liquid interface exhibited a typical dendritic growth morphology, with primary dendrites protruding from the solid phase to the liquid phase, and the degree of directional growth was high ($\theta=3.1^\circ$) (Fig. 6(a)). For directional solidification at (5.31 T, 0 T²/m), the alloy exhibited a typical flat interface eutectic growth morphology at the solid/liquid interface (Fig. 6(b)). When a gradient magnetic field (5.31 T, -30 T²/m) was applied, primary dendrites appeared at the solid/liquid interface, and the degree of directional growth was lower ($\theta=18.5^\circ$) than for directional solidification at (5.31 T, 0 T²/m) (Fig. 6(c)). However, with the increase of the field gradient to 70 T²/m, the directional growth of the dendrites at the front of the solid/liquid interface became regular and the degree of

directional growth increased ($\theta=4.51^\circ$) (Fig. 6(d)).

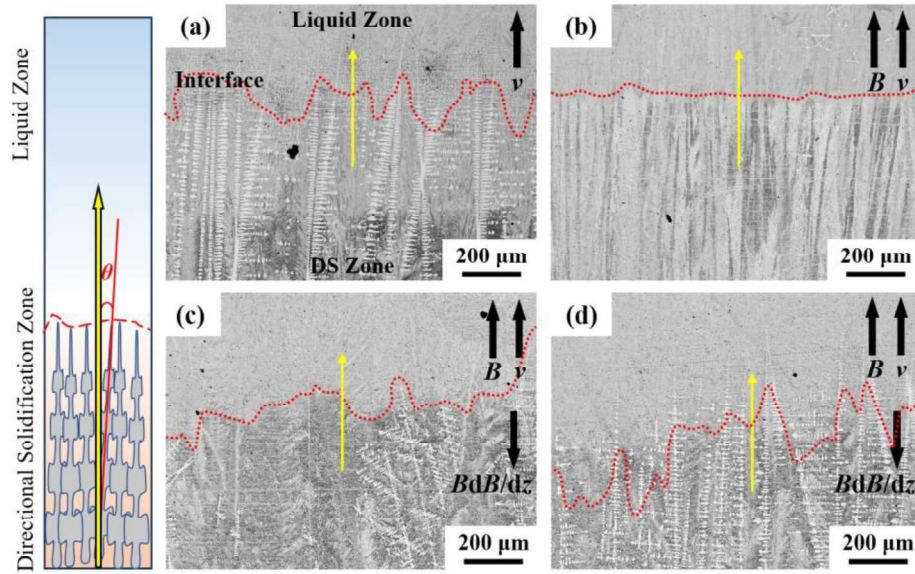


Fig. 6 Microstructure of the solid/liquid interface of the Cu-73.4 wt.% Ag alloy directional solidified under different magnetic fields: (a) (0 T, 0 T²/m), (b) (5.31 T, 0 T²/m), (c) (5.31 T, -30 T²/m), and (d) (5.31 T, -70 T²/m).

EPMA line scanning analysis was performed along the directions of the yellow lines in Fig. 6, and the results are shown in Fig. 7. Without magnetic field, the Cu solute distribution along the directional solidification direction was relatively uniform (Fig. 7(a)). While with a uniform magnetic field, the Cu solute content showed an obvious peak in the liquid near the solid/liquid interface, and it wildly fluctuated in the liquid zone at (5.31 T, 0 T²/m) (Fig. 7(b)). With a low gradient magnetic field (5.31 T, -30 T²/m), the distribution of the Cu solute in the solid front and liquid zone was more uniform than that of without magnetic field case (Fig. 7(c)). With a high gradient magnetic field (5.31 T, -30 T²/m), the Cu solute in the liquid near the solid/liquid interface was lower than that of without magnetic field case (Fig. 7(d)).

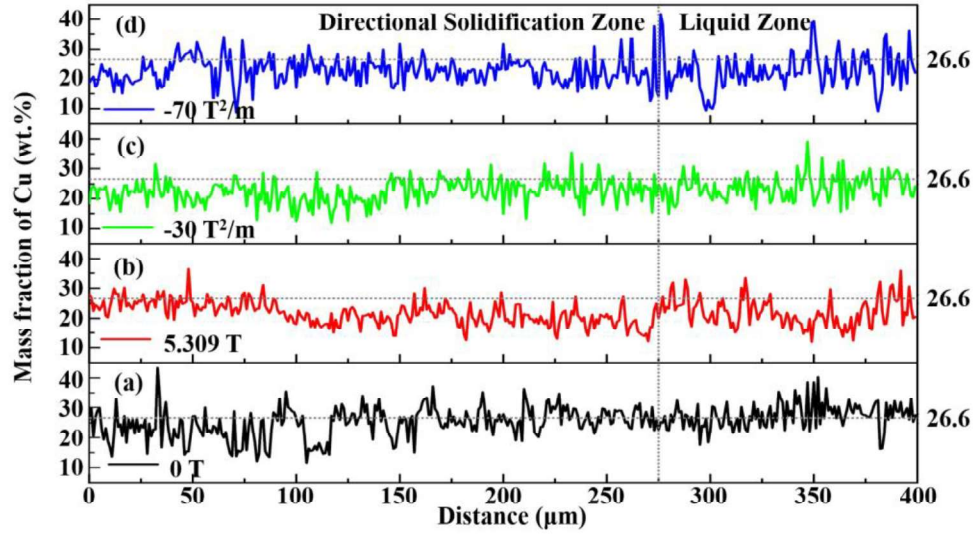


Fig. 7 EPMA line scanning of the solid/liquid interface of the Cu-73.4 wt.% Ag alloy directional solidified under different magnetic fields: (a) (0 T, 0 T²/m), (b) (5.31 T, 0 T²/m), (c) (5.31 T, -30 T²/m), and (d) (5.31 T, -70 T²/m).

To study the solute distribution at a smaller scale, EPMA mapping analysis of the dendritic or eutectic growth tips at the solid/liquid interface was performed (Fig. 8). The mapping images reflected the distribution of the Cu solute. For directional solidification at (0 T, 0 T²/m), the dendritic growth accumulated a large amount of the Cu solute at the interface front, and the distribution was relatively uniform (Fig. 8(a1)). When a uniform magnetic field (i.e., (5.31 T, 0 T²/m)) was applied, the high magnetic field significantly changed the solute distribution at the tip of the dendrites, resulting in solute interception at the interface front. The Cu solute aggregated in blocks at the interface front, and a clear Cu enrichment zone appeared horizontally, as indicated by the red circle in Fig. 8(b1). Under a gradient magnetic field, the Cu solute accumulated near the dendritic tip, but the degree of aggregation was significantly poorer than for directional solidification at 0 T. As the absolute value of the magnetic field gradient increased, the degree of Cu solute aggregation increased (Fig. 8(c1)–(d1)). For directional solidification at 0 T, the distribution of the Cu solute at the front of the alloy solid/liquid interface was relatively stable, while there was partial enrichment in certain areas under a uniform magnetic field. As the magnetic field gradient increased, the Cu solute returned to a uniform distribution, but the solute content was lower than that for

directional solidification at 0 T.

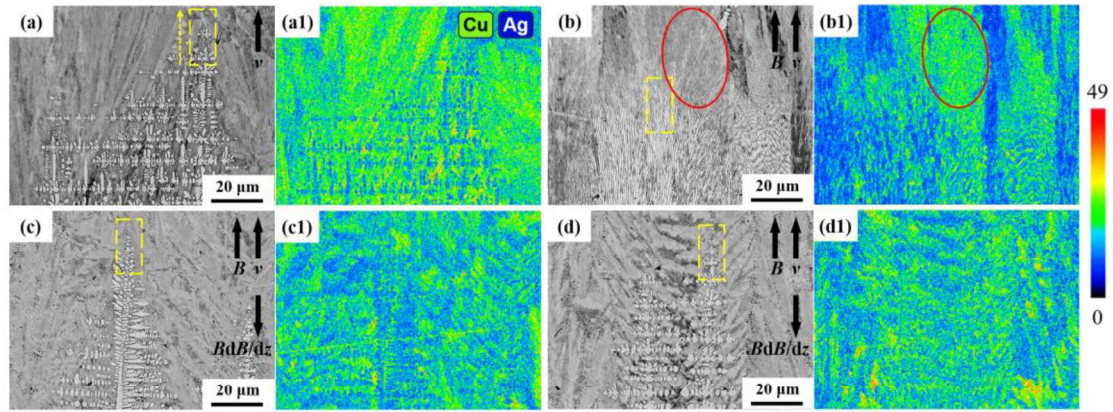


Fig. 8 SEM images and EPMA map of the solid/liquid interface of the Cu-73.4 wt.% Ag alloy directionally solidified under different magnetic fields: (a) and (a1) (0 T, 0 T²/m), (b) and (b1) (5.31 T, 0 T²/m), (c) and (c1) (5.31 T, -30 T²/m), and (d) and (d1) (5.31 T, -70 T²/m).

To accurately investigate the migration of Cu in the solute diffusion layer at the front of the solid/liquid interface, EPMA point scanning analysis of the dendritic tips in the yellow boxes in Fig. 8(a)–(d) was performed. The precise compositions of 15 points were measured with a step size of 1 μm, and the results are shown in Fig. 9(a). For directional solidification at (5.31 T, 0 T²/m), the content of Cu atoms in the solute diffusion layer increased, while a gradient magnetic field decreased the content of Cu. The solute content in the solid phase did not significantly fluctuate, while the Cu content in the liquid phase significantly decreased at positions far from the solute diffusion layer. The solute contents in the solid and liquid phases are given in Table 1, and the calculated solute diffusion coefficients at the front of the solid/liquid interface are shown in Fig. 9(b). Applying a magnetic field increased the solute diffusion coefficient, and the solute diffusion coefficient increased with increasing absolute value of the magnetic field gradient.

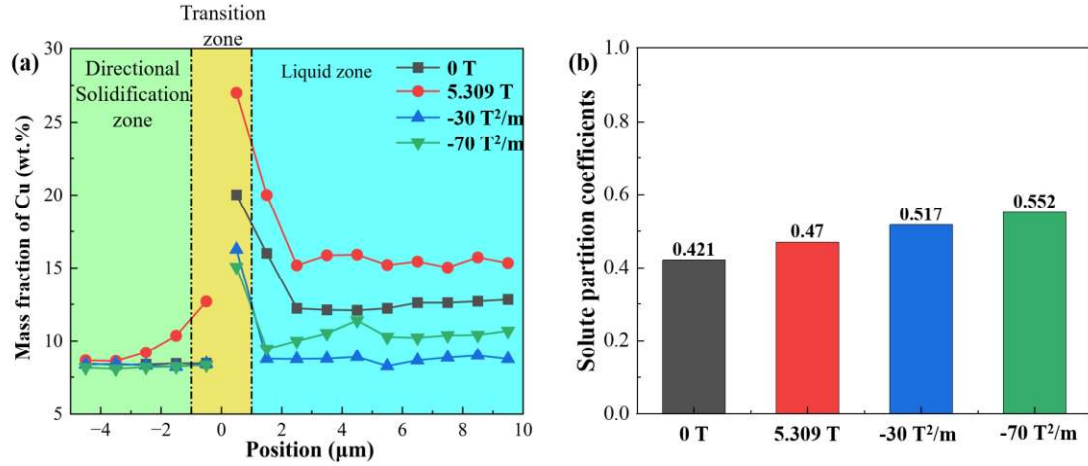


Fig. 9 (a) Mass fraction of Cu and (b) solute partition coefficients of the solid/liquid interface of the Cu-73.4 wt.% Ag alloy directionally solidified under different magnetic fields.

Table 1 Solute content and solute partition coefficients of the solid/liquid interface of the Cu-73.4 wt.% Ag alloy directionally solidified under different magnetic fields.

	0 T, 0 T ² /m	5.039 T, 0 T ² /m	5.31 T, -30 T ² /m	5.31 T, -70 T ² /m
C_S	8.436	12.686	8.415	8.321
C_L	20.021	27.002	16.261	15.068
$K_{Cu}=C_S/C_L$	0.421	0.470	0.517	0.552

Previous studies [26] have indicated that during the directional solidification of alloys in the absence of a magnetic field, Cu-Ag alloys tend to grow in dendrite morphology as shown in Figs. 3(a) and 10(a). But the phenomenon changed after applying the magnetic field. Previous studies [29] have indicated that uniform magnetic fields can affect the convection and solute migration during solidification processes by Lorentz forces and thermoelectric magnetic force. With the increase of magnetic flux density, the effect of thermoelectric magnetic force would compete with the Lorentz force, and the ratio would increase first and then decrease [27,28]. In this work, the magnetic flux density was 5.31 T, which is a relatively high value. Therefore, the Lorentz force played the main role during directional solidification. At (5.31 T, 0 T²/m), the Lorentz force suppressed the melt convection, causing the solute enrichment at the front of solid-liquid interface (Fig. 7(b)). Also, the lateral diffusion of Cu in the solute diffusion layer was suppressed, causing Cu to intermittently aggregate, as shown by the red circle in Fig. 8(b1). Thus, the component changed from C_1 to C_2 (as shown in Figs. 9(a) and

10(d)), and the solidification reaction shifted from a hypereutectic reaction to a eutectic reaction (Figs. 3(b) and 10(b)).

With a gradient magnetic field, except for the Lorentz force, the alloy was also acted upon by the magnetization force. As soon as the Cu solute enrichment formed at the front of solid-liquid interface caused by the Lorentz force, the migration of the Cu solute was promoted by the magnetization force. Considering the fact that Cu is antimagnetic and was under a negative gradient magnetic field, the Cu solute moved upward in the front of the solid-liquid interface, which reduces the Cu content (Fig. 10(c)). Then, the component of the Cu decreased back from C_2 to C_3 , and the corresponding solidification temperature increases from T_2 to T_3 , which leads to constitutional undercooling at the solid/liquid interface (Fig. 10(d)). Thus, the re-nucleation of the primary Ag phase was promoted. The re-nucleation of the primary Ag phase resulted in a reduced degree of directional growth of the primary Ag dendrites (Fig. 3(c) and (d)). With the increase of the magnetic field gradient, the component of the Cu further decreased from C_3 to near C_1 (Fig. 10(d)).

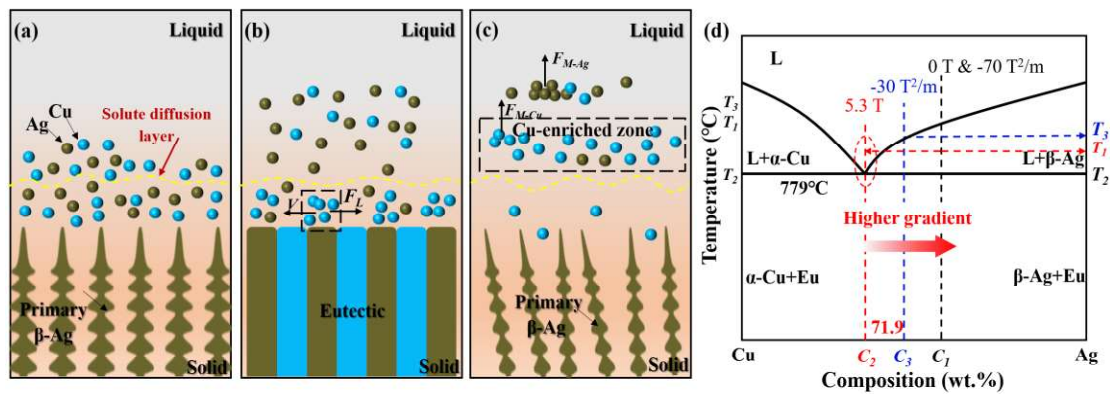


Fig. 10. Schematic diagrams of the solute migration at the solid/liquid interface during the directional solidification of the Cu-73.4 wt.% Ag alloy under various magnetic fields: (a) without magnetic field; (b) with a uniform magnetic field; (c) with a gradient magnetic field; (d) phase diagram under a gradient magnetic field.

4. Conclusion

In this work, directional solidification experiments of a Cu-73.4 wt.% Ag alloy have

1 been conducted under different gradient magnetic fields. The effects of gradient
2 magnetic fields on the solute migration and microstructure evolution of the alloys have
3 been investigated. The main conclusions are as follows:
4

5
6 (1) Without magnetic field, the alloy showed an aligned dendritic microstructure. Under
7 a uniform magnetic field, the dendritic microstructure transformed to a eutectic
8 morphology. Under a gradient magnetic field, the alloy exhibited again the dendritic
9 microstructure, but with poor alignment.
10

11
12 (2) The microstructure transformation from aligned dendritic to eutectic under the
13 uniform magnetic field can be attributed to the interception of the Cu solute at the
14 solid/liquid interface caused by the Lorentz force. While, the microstructure
15 transformation from eutectic to poor aligned dendritic morphology under the gradient
16 magnetic field can be attributed to the upward migration of the Cu solute driven by the
17 magnetization force.
18
19
20
21
22
23
24
25
26

27 **Acknowledgments**

28
29 This work was supported by the National Natural Science Foundation of China (Grant
30 Nos. U2241230 and 52127807).
31
32
33
34
35
36

37 **Data availability**

38
39 The data that support the findings of this study are available from the corresponding
40 author upon reasonable request.
41
42
43
44

45 **Declarations**

46 **Conflict of interest**

47
48 The authors declare that they have no known competing interests for the work reported
49 in this paper.
50
51
52
53

54 **Ethical approval**

55
56 This work does not require any ethical statement.
57
58
59
60
61
62
63
64
65

References

- [1] Tang Y, Wu Y, Zhang Y, Dai YB, Dong Q, Han YF, Zhu GL, Zhang J, Fu YA, Sun BD (2021) Intermittent nucleation and periodic growth of grains under thermo-solutal convection during directional solidification of Al-Cu alloy. *Acta Mater* 212:116861. <https://doi.org/10.1016/j.actamat.2021.116861>
- [2] Zhang WQ, Fu H, Yang YS, Hu ZQ (1998) A numerical model for spacing selection of lamellar eutectics grown from flowing liquids. *J Cryst Growth* 194:263-271. [https://doi.org/10.1016/S0022-0248\(98\)00481-3](https://doi.org/10.1016/S0022-0248(98)00481-3)
- [3] Yan J, Liu T, Wang MM, Sun JM, Dong SL, Zhao LJ, Wang Q (2022) Constitutional supercooling and corresponding microstructure transition triggered by high magnetic field gradient during directional solidification of Al-Fe eutectic alloy. *Mater Charact* 188:111920. <https://doi.org/10.1016/j.matchar.2022.111920>
- [4] Mullins WW, Sekerka RF (1964) Stability of a planar interface during solidification of a dilute binary alloy. *J Appl Phys* 35:444-451. <https://doi.org/10.1063/1.1713333>
- [5] Ma CZ, Zhang RJ, Li ZX, Jiang X, Wang YW, Zhang C, Yin HQ, Qu XH (2022) Solidification shrinkage and shrinkage-induced melt convection and their relation with solute segregation in binary alloys. *Comput Mater Sci* 215:111815. <https://doi.org/10.1016/j.commatsci.2022.111815>
- [6] Long ZP, Wang JT, Yan S, Yu X, Hou L, Li X (2024) Experimental determination of solid-liquid interface energy for para- and diamagnetic solid solution in equilibrium with eutectic liquid under a high magnetic field. *J Alloys Compd* 971:172694. <https://doi.org/10.1016/j.jallcom.2023.172694>
- [7] Wang B, Li GX, Wang Y, Su YT, Sun HL, Guo ZH, Zhang D, Dong ZQ (2021) Characterization of the Fe-6.5 wt% Si strip with rapid cooling coupling deep supercooled solidification. *ACS Omega* 6:25412-25420. <https://doi.org/10.1021/ACSOMEGA.1C03367>
- [8] Yan N, Wang ZH, Ruan Y, Wei BB (2019) Solute redistribution and micromechanical properties of rapidly solidified multicomponent Ni-based alloys. *Sci*

China Technol Sci 62:472-477. <https://doi.org/10.1007/S11431-018-9411-Y/METRICS>

[9] Du DF, Fautrelle Y, Dong AP, Shu D, Zhu GL, Sun BD, Nguyen-Thi H, Ren ZM, Li X (2018) In-situ fabrication of graded material with the application of a horizontal magnetic field during directional solidification. *Mater Charact* 141:423-432. <https://doi.org/10.1016/J.MATCHAR.2018.05.007>

[10] Lin WH, Zhou BF, Zheng TX, Shi PJ, Shen Z, Li Q, Ren WL, Zhang L, Zhang QJ, Zhong YB (2023) X-Ray tomographic quantification of diffusive growth of metallic dendrite in high magnetic field. *Metall Mater Trans A Phys Metall Mater Sci* 54:4295-4305. <https://doi.org/10.1007/s11661-023-07164-z>

[11] Zhong QD, Zhong HY, Han HB, Shu MY, Hou L, Zhu YY, Li X (2022) Formation mechanism of ring-like segregation and structure during directional solidification under axial static magnetic field. *J Mater Sci Technol* 99:48-54. <https://doi.org/10.1016/j.jmst.2021.05.050>

[12] Battesti R, Beard J, Böser S, Bruyant N, Budker D, Crooker SA, Daw EJ, Flambaum VV, Inada T, Irastorza IG, Karbstein F, Kim DL, Kozlov MG, Melhem Z, Phipps A, Pagnat P, Rikken G, Rizzo C, Schott M, Semertzidis YK, Kate HT, Zavattini G (2018) High magnetic fields for fundamental physics. *Phys Rep* 765-766:1-39. <https://doi.org/10.1016/j.physrep.2018.07.005>

[13] Liu T, Wang Q, Yuan Y, Wang K, Li G (2018) High-gradient magnetic field-controlled migration of solutes and particles and their effects on solidification microstructure: A review. *Chin Phys B*, 27: 118103. <https://doi.org/10.1088/1674-1056/27/11/118103>

[14] Keigo Hoshikawa (1982) Czochralski Silicon Crystal Growth in the Vertical Magnetic Field. *Jpn J Appl Phys* 21: L545. <https://doi.org/10.1143/JJAP.21.L545>

[15] Li X, Gagnoud A, Fautrelle Y, Ren ZM, Moreau R, Zhang Y, Esling C (2012) Dendrite fragmentation and columnar-to-equiaxed transition during directional solidification at lower growth speed under a strong magnetic field. *Acta Mater*, 60(8): 3321-3332. <https://doi.org/10.1016/j.actamat.2012.02.019>.

- [16] Wang J, Fautrelle Y, Ren ZM, Nguyen-Thi H, Salloum G, Reinhart G, Mangelinck-Noël N, Li X, Kaldre I (2014) Thermoelectric magnetic flows in melt during directional solidification. *Appl Phys Lett* 104: 121916. <https://doi.org/10.1063/1.4870099>.
- [17] Liu T, Wang Q, Gao A, Zhang C, Wang CJ, He JC (2007) Fabrication of functionally graded materials by a semi-solid forming process under magnetic field gradients. *Scr Mater* 57:992-995. <https://doi.org/10.1016/j.scriptamat.2007.08.011>
- [18] Sun JM, Liu T, Guo X, Yuan S, Wang J, Hirota N, Wang Q (2024) Effect of a high-gradient magnetic field on grain refinement of a hypoeutectic Mn-Sb alloy during directional solidification. *J Mater Sci Technol* 175:47-54. <https://doi.org/10.1016/j.jmst.2023.07.037>
- [19] Tu S, Mai Y, Tong Y, Liu T, Dong M, Wang Q (2018) Enhancement of magnetostrictive performance of Tb_{0.27}Dy_{0.73}Fe_{1.95} by solidification in high magnetic field gradient. *J Alloy Comp* 741: 1006-1011. <https://doi.org/10.1016/j.jallcom.2018.01.215>.
- [20] Lin WH, Zhou BF, Liu Y, Guo XH, Zheng TX, Zhong YB, Zhang L, Zhang QJ Wang QL (2022) Dendrite morphology in Al-20 wt% Cu hypoeutectic alloys in 24 T high magnetic field quantified by ex-situ X-ray tomography. *J Alloys Compd* 918:165679. <https://doi.org/10.1016/j.jallcom.2022.165679>
- [21] Hu SD, Hou L, Wang K, Liao ZM, Zhu W, Yi AH, Li WF, Fautrelle Y, Li X (2021) Effect of transverse static magnetic field on radial microstructure of hypereutectic aluminum alloy during directional solidification. *J Mater Sci Technol* 76:207-214. <https://doi.org/10.1016/j.jmst.2020.11.025>
- [22] Liu T, Wang Q, Wang CJ, Li HT Wang ZY, He JC (2011) Effects of high magnetic fields on the distribution and alignment of primary phases in an Al-12Si-11.8Mg-6.5Ti alloy. *Metall Mater Trans A Phys Metall Mater Sci* 42: 1863-1869. <https://doi.org/10.1007/S11661-010-0569-8/FIGURES/6>
- [23] Yan J, Liu T, Sun J, Zhang S, Guo X, Yuan S, Wang Q (2025) Microscopic Mechanisms of Solute Migration and Redistribution at the Solid-Liquid Interface During Directional Solidification of a Cu–Ag Eutectic Alloy Under High Magnetic

Fields. Metall Mater Trans A Phys Metall Mater Sci 56: 400-413.
<https://doi.org/10.1007/s11661-024-07654-8>.

[24] Hansen M, Anderko K, Salzberg HW (1958) Constitution of binary alloys. J. Electrochem Soc 105:260C. <https://doi.org/10.1149/1.2428700>

[25] Wu MX, Liu T, Dong M, Sun JM, Dong SL, Wang Q (2017) Directional solidification of Al-8 wt.%Fe alloy under high magnetic field gradient. J Appl Phys 121: 064901. <https://doi.org/10.1063/1.4975675>.

[26] Biesuz M, Sauders T, Ke D, Reece M, Hu C, Grasso S (2020) A review of electromagnetic processing of materials (EPM): heating, sintering, joining and forming. J Mater Sci Technol 69: 239-272. <https://doi.org/10.1016/j.jmst.2020.06.049>.

[27] Li X, Fautrelle Y, Ren Z (2007) Influence of thermoelectric effects on the solid-liquid interface shape and cellular morphology in the mushy zone during the directional solidification of Al-Cu alloys under a magnetic field. Acta Mater 55:3803-3813. <https://doi.org/10.1016/j.actamat.2007.02.031>

[28] Yan JG, Liu T, Liao J, Sun JM, Guo XY, Ren ZM, Wang Q (2021) Microstructural evolution and solute migration in the mushy zone of peritectic Al-18 at. pct Ni alloy in high magnetic fields. Metall Mater Trans A Phys Metall Mater Sci 52:726-740. <https://doi.org/10.1007/s11661-020-06116-1>

[29] Xiao YB, Liu T, Tong YX, Dong M, Li JS, Wang J (2021) Microstructure evolution of peritectic Al-18 at.% Ni alloy directionally solidified in high magnetic fields. J Mater Sci Technol 76:51-59. <https://doi.org/10.1016/j.jmst.2020.11.004>